IEEE Access
Multidisciplinary | Rapid Review | Open Access Journal

Received February 6, 2019, accepted February 27, 2019, date of current version April 15, 2019.

Digital Object Identifier 10.1109/ACCESS.2019.2905726

Design and Performance Analysis of Low Pull-In Voltage of Dimple Type Capacitive RF MEMS Shunt Switch for Ka-Band

K. GIRIJA SRAVANI[1,2], D. PRATHYUSHA[1], K. SRINIVASA RAO[2], (Member, IEEE), P. ASHOK KUMAR[1], G. SAI LAKSHMI[1], CH. GOPI CHAND[1], P. NAVEENA[1], LAKSHMI NARAYANA THALLURI[1], AND KOUSHIK GUHA[2]

[1]MEMS Research Center, Department of Electronics & Communication Engineering, Koneru Lakshmaiah Education Foundation, Guntur 522502, India
[2]National MEMS Design Center, Department of Electronics & Communication Engineering, National Institute of Technology, Silchar 788010, India

Corresponding author: K. Girija Sravani (e-mail: kondavitee.sravani03@gmail.com)

ABSTRACT This paper deals with the study of dimple type RF MEMS capacitive shunt switch using different meandering techniques for high isolation and low actuation voltage. The novelty of the proposed RF MEMS switch is it incorporates the meanders and dimples, which help to reduce the actuation voltage. The proposed switch structure is optimized, designed, and simulated with FEM analysis such as electromechanical and electromagnetic by using COMSOL and HFSS tools respectively. The best performance of the switch is observed by varying different parameters such as beam material, beam thickness, dielectric thickness, and airgap. The proposed switch with different meandering techniques attains the pull-in voltage in the range of 10.3–46 V, particularly the three uniform meander technique has low actuation voltage of 10.3 V. The RF performance of the device is particularly tuned in the range of 26.5–40 GHz frequency range and it is analyzed for all types of meanders. Among them, the non-uniform single meander has attained the best isolation of −54.13 dB at 40 GHz in the off state. The insertion and return losses of the device are −0.514 dB and −17.35 dB over 1-40 GHz frequency in on state.

INDEX TERMS RF MEMS, pull-in-voltage, capacitance ratio, dimples, switching time, insertion loss, isolation, return loss.

I. INTRODUCTION

MEMS technology based RF switches are emerges in high frequency communication applications. MEMS technology has the pretty much competition with solid state technology switches, but at high frequency range in the aspect of isolation and insertion behaviour of MEMS RF switches shows a great potential [1]. A low power consumption nature of RF MEMS switches attracting the researchers in communication industry to design the devices for 5G applications [2]. Low pull-in voltage and high isolation are the two significant research challenges in design and fabrication aspects of capacitive RF MEMS switches [3]. The serpentine structure meander helps to reduce the pull-in voltage of the switch [4]–[9]. To overcome the switch geometry and RF performance parameter challenges in the above-mentioned literature, the proposed device is selected, and it consists of semicircular arc shaped curves on either side of the switch having different flexures such as uniform and non-uniform meanders along with the etching holes created on the beam. The proposed capacitive dimple type novel switch is optimized with the bottom-up approach in order to tune the switch to operate at Ka band applications. The optimized dimensions of the switch geometry can be helpful to tune the frequency. The proposed capacitive dimple type switch is designed with uniform and non-uniform meandering techniques. The proposed switch is analyzed applying electromechanical study by varying gap between the electrodes, beam materials and materials of the switch. The switching time analysis is also done for the proposed switch as it is important factor to understand the transition time from on state to off state in the micro level. The switching time analysis are tabulated for different meandering techniques. It is necessary to carry out stress analysis by applying uniform distribution of force on the beam. Capacitance analysis is evaluated for the proposed dimple type switch to maintain minimum capacitance to pass high

The associate editor coordinating the review of this manuscript and approving it for publication was Bora Onat.

frequency in the switches. RF performance includes insertion loss, return loss and isolation. From the mentioned results it is observed that the non-uniform one meander shows good performance at 40 GHz frequency. Therefore, the proposed novel type dimple type RF MEMS switch can be used at Ka-band applications.

This paper is organized as follows, in Section II, the outlines of the design specifications of the proposed switch is presented. In Section III, the theoretical aspects of RF MEMS are discussed. In Section IV, the simulation of electromechanical and electromagnetic analysis of the proposed device are discussed. Finally, Section V is concluded at the end of the paper.

II. DETAILS OF THE PROPOSED RF MEMS SWITCH

A. CONVENTIONAL FIXED – FIXED SWITCH: WORKING MECHANISM

In RF MEMS devices, most of preferred switches are fixed-fixed capacitive shunt switches. The schematic view of the fixed-fixed shunt type switch is shown in Figure 1. This device consists of a beam, oxide layer, two anchors, dielectric layer, and a CPW transmission line which in turn consists of two ground planes and signal line.

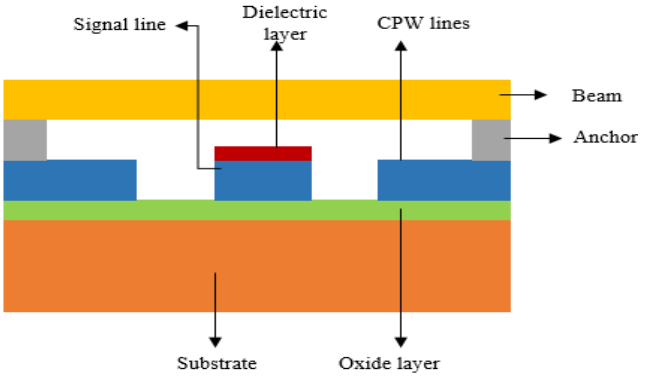

FIGURE 1. Schematic view basic fixed-fixed beam rf mems structure.

The dielectric layer is placed over the transmission line, which forms a capacitor in between the beam and the signal line. In OFF state, the capacitance developed due to actuated beam generates a short resistive path from the signal line to the ground and accordingly it bypass the transmission of RF signal to ground. In ON state position of the switch, RF signal is transmitted along the CPW line with a minimum capacitance in between the beam and the signal line. The OFF state and ON state schematic view of capacitive RF MEMS Switch is as shown in Figure 2. A DC voltage is applied to the beam to create a electric field, which ultimately forms an electrostatic force to pull the beam downwards onto the dielectric layer. The switch behaves as a pure capacitor in onstate and in offstate it depends on the frequency of the transmitting signal. If $f < f_0$, it acts as pure capacitor, pure resistor when $f=f_0$ and it acts as a pure inductor when $f > f_0$.

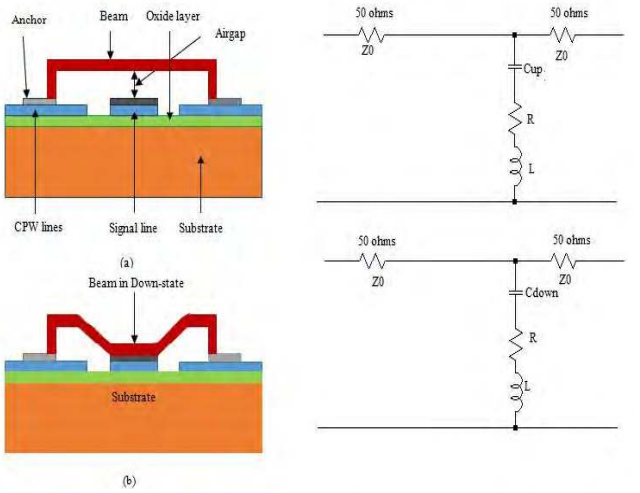

FIGURE 2. Schematic view of rf mems switch (a) on state (b) off state.

B. THE STRACTURE OF PROPOSED SWITCH

In this paper, a low pull–in voltage of capacitive RF MEMS switch is proposed along with perforations and meanders. The proposed capacitive RF MEMS switch is designed over a substrate made up of semiconductor material. Oxide layer is preferred in between the transmission line and the substrate to reduce the DC loss. The switch is made up of thin metallic beam with the both ends are fixed to the ground lines of the CPW. The dielectric layer is placed above the signal line to develop the capacitance. Anchors are placed above the ground lines of a CPW line where these are used to hold the beam through meanders. A semi-circular disc shape is selected as an anchor to hold the beam efficiently without having any displacement due to acceleration due to gravity. This proposed switch is designed with single, double, three uniform and non-uniform meandering techniques.

C. DIMPLES

Dimple is also known as perforations and are incorporated on the beam to reduce the residual stress. It improves the performance parameters like pull-in voltage, flexibility, switching speed, squeezing film damping and reliability of a switch. The beam is displaced vertically towards the substrate during an electrostatic pull-down actuation and the air gap between the dielectric layer and the beam decreases causing air to be squeezed. The dimples will reduce the mass of the beam which helps to reduce the effect of spring constant. The hole shows a great impact on up-state capacitance and its negligible if the diameter of the holes is less than $3\text{-}4g_0$. The dimples are not only used to bend the beam but also helps to regain its original position when the DC is removed which improves releasing time. The circular type of dimples are chosen for different meander of the proposed structure as shown in the figure 3.

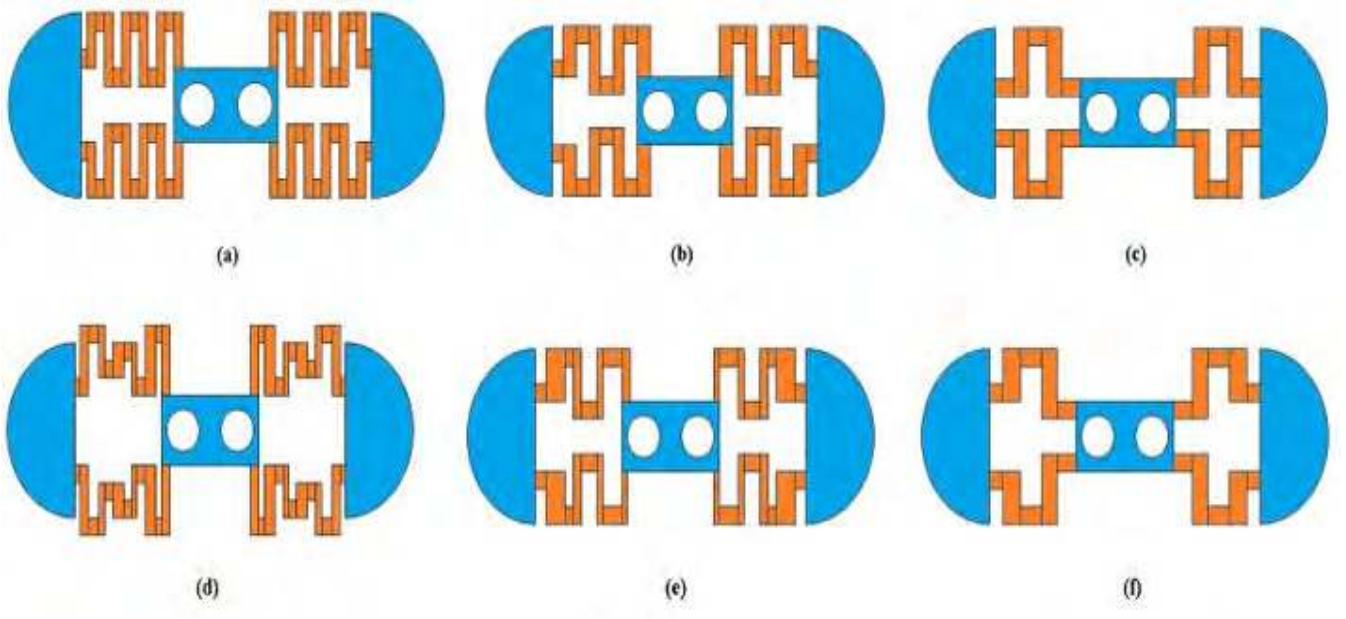

FIGURE 3. Design shows three meanders (a) three uniform meander (b) two uniform meander (c) single uniform meander (d) three non-uniform meander (e) two non-unifrom meander and (f) single non-uniform meander in proposed switches.

D. MEANDERS

Meandering technique is used to increases the switching speed and reduces the actuation voltage by decreasing spring constant. In this proposed switch comparative analysis is done for different meandering techniques. The meandering techniques includes uniform and non-uniform structures containing one, two and three meanders. The uniform and non-uniform meanders are shown in Figure 3, which shows the series combinations blocks to form meanders decreases the spring constant.

E. DIMENSIONS OF PROPOSED SWITCH

Quartz material is used for a substrate with relative permitivity ($\mathcal{E}_r$) as 3.8. Oxide layer is made up of Silicon dioxide (SiO_2) and to analyse performance of switch the CPW and beam materials are varied as gold (Au), titanium (Ti), platinum (Pl) and indium (In). Gold is preferred as best choice because of the high conductivity and less reactive with the other materials. The dielectric layer is made up of AlN (Aluminum Nitride) because of its better capacitance effect than the Si_3N_4(Silicon Nitride). The dimensions and materials for the proposed switch is shown in Table 1.

TABLE 1. Dimensions of proposed rf mems switch.

Parameters	Length	Width	Thickness	Materials
Substrate	380 µm	400 µm	25 µm	Quartz,Si,Ge
CPW (G)	140 µm	400 µm	20 µm	Au,Ti,Pl,In
CPW(S)	60 µm	400 µm	20 µm	Au,Ti,Pl,In
Anchor	30 µm	60 µm	1 µm	Gold
Dielectric	60 µm	60 µm	0.1µm	AlN,Si_3N_4
Beam	36 µm	20 µm	1 µm	Au,Ti,Pl,In

Si = Silicon, Ge = Germanium.

III. THEORETICAL ANALYSIS

A. SPRING CONSTANT

The mechanical behaviour of RF MEMS switch is mostly depends on the spring constant developed by the meandears. In RF MEMS switches, the meanders develop the inductance due to overlapping with the ground planes. These meanders increases the quality of the transmitting signal by decreasing the insertion loss and increasing isolation. Each meander comprises of rectangular blocks and the spring constant of the each block is given by [10].

$$K = \frac{Ewt^3}{l^3} \tag{1}$$

where,

E = young's modulus, w = width of the block,

t = thickness of the block, l = length of the block.

Each block in the non-uniform meander section varies with the dimensions which are shown in Table 2 and the block in uniform meanders are in same length which are separated by the identical span blocks.

TABLE 2. Dimensions of spring constant for different meanders.

Spring Constant	Three Meanders				Two Meanders		Single Meander			
	uniform		non-uniform		uniform		uniform		non-uniform	
(µm)	l	w	l	w	l	w	l	w	l	w
K_{s1}	5	2	6	2	5	4	7	5	5	5
K_{s2}	15	3	20	3	15	5	20	5.5	15	6.5
K_{s3}	5	3	5	4	5	5	7	5	8	5
K_{s4}	20	3	15	2	20	4	20	5.5	20	5.5

The formula for spring constant of each meander is denoted as K_m and is given by

$$\frac{1}{K_m} = \frac{1}{K_1} + \frac{1}{K_2} + \frac{1}{K_3} \tag{2}$$

where,
K_1, K_2 and K_3 are the stifness of each blocks in meanders. The overall spring constant (K_s) of the actuation mechanism is expressed as

$$K_s = 4K_m \tag{3}$$

Hence the spring constant is multiplied with 4 because the beam is suspended by four meanders on either side.

Spring constant is mainly depends on the young's modulus (E) and thickness of the beam. Young's modulus of the gold material is 78 GPa, titanium is having 116 GPa and platinum has 168 GPa. The spring constant of the different meanders have been evaluated and presented in Table 3.

TABLE 3. Spring constant of different beam materials for both uniform and non-uniform meanders.

Materials	Meanders			
	Uniform		Non-uniform	
	Three	single	Three	single
Gold	21.2 N/m	96.3 N/m	24.9 N/m	129 N/m
Titanium	31.8 N/m	141.7 N/m	37.4 N/m	190 N/m
Platinum	50.9 N/m	227.3 N/m	59.8 N/m	310 N/m

B. ACTUATION VOLTAGE

Electrostatic actuation has been utilized to change the mode of operation of the switch i.e., from ON to OFF state. MEMS shunt switch utilizes a DC voltage to be actuate it, and the voltage which is allowed to contact perfectly the dielectric layer and the beam is known as pull-in-voltage and it is given as [11].

$$V_p = \sqrt{\frac{8K_s g_0^3}{27\varepsilon_0 (A - A_d)}} \tag{4}$$

where,
K_s is spring constant for bridge structure, $g_0$is air gap between the beam and dielectric, $\mathcal{E}_0$ is a relative permittivity of free space value is $8.854E - 12$,

$$A = l * w \tag{5}$$

where,
l is length of the beam, w is width of the beam and A is area of the beam, A_d is area of the dimples present in the switch.

$$A_d = 2(\pi r^2) \tag{6}$$

where,
r is radius of the circular perforation which is taken as 6μ m. In this proposed switch, we have used two dimples, thus the total area occupied by the dimples is two times of the A_d mentioned in the equation 6.

1) IMPACT ON BEAM MATERIALS

Pull-in-voltage of the switch is directly proportional to spring constant offered by the meanders. The pull-in voltage of the switch is calculated for different materials. The variation in the spring constant for different materials is due to change in young's modulus. Below Table 4, shows that the properties of the beam materials which shows highly impact on spring constant and pull-in-voltage.

TABLE 4. Pull-in-voltage of different beam materials for both uniform and non-uniform meanders.

Materials	Meanders			
	Uniform		Non-uniform	
	Three	Single	Three	single
Gold	10.3 V	36.5 V	11.6 V	46.04 V
Titanium	12.6 V	44.3 V	14.2 V	55.9 V
Platinum	15.9 V	56.13 V	17.9 V	71.4 V

We observed that, among different meandering techniques the obtained best pull-In-voltage is as low as 10.3 volts for three uniform meandering technique which is having spring constant of 21.2 N/m.

2) IMPACT ON AIR GAP

The variation of the pull-in-voltage at different airgaps is tabulated in table 5. Pull-in-voltage is directly proportional to air gap of the beam. By changing the air gap such as 0.9 μm, 1 μm, 1.2 μm and 1.5 μm then pull-in-voltage is also varies and shown in Table 5. We observed that among the all meandering techniques, three uniform meanders exhibits best pull-in-voltage when compare with non-uniform meander. From the Figure III, IV and V it is observed that the pull in voltage is less for lesser air gap and low young's modulus materials having low spring constant.

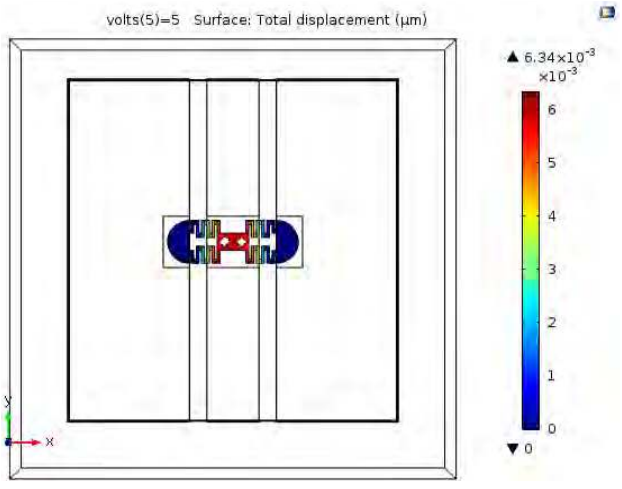

FIGURE 4. Voltage versus displacement of a proposed switch with semi circular disc using three unifrom meanders.

3) IMPACT ON BEAM THICKNESS

The thickness of the beam in the switch is directly proportional to spring constant, therefore, pull-in-voltage is also

TABLE 5. Different airgaps for different materials of uniform and non-uniform meanders.

Meanders	Air gap	Gold	Titanium	Platinum
Uniform 3 meanders	0.9 μm	10.31 V	12.6 V	15.9 V
	1 μm	12 V	15 V	19 V
	1.2 μm	15.8 V	19.4 V	24.5 V
	1.5 μm	22 V	27 V	34 V
Non-uniform 3 meanders	0.9 μm	12 V	14 V	18 V
	1 μm	14 V	17 V	21 V
	1.2 μm	18 V	22 V	28 V
	1.5 μm	25 V	30.5 V	38.5 V
Uniform single meander	0.9 μm	36.5 V	44.3 V	56.1 V
	1 μm	42.78 V	51.91 V	65.7 V
	1.2 μm	56.24 V	68.24 V	86.42 V
	1.5 μm	78.59 V	95.37 V	120.8 V
Single non-uniform meanders	0.9 μm	46.04 V	55.9 V	71.4 V
	1 μm	53.93 V	65.5 V	83.6 V
	1.2 μm	70.89 V	86.13 V	109.9 V
	1.5 μm	99.07 V	120.4 V	153.6 V

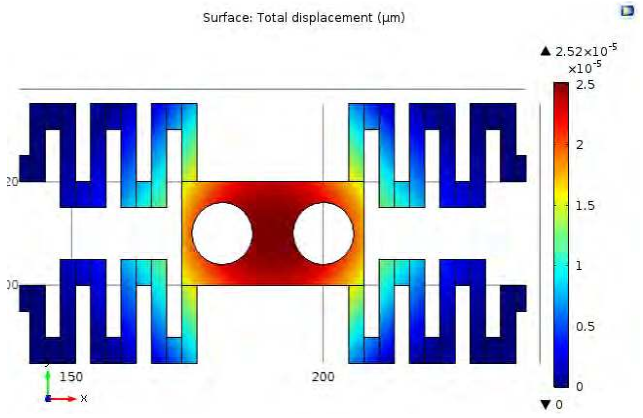

FIGURE 5. Voltage versus displacement of a proposed switch without semi circular disc using three unifrom meanders.

depending on the thickness of the beam. Then the different thickness of the beam for both meandering techniques are shown in Table 6 and Table 7.

C. VON MISES STRESS AND DEFLECTION DUE TO RESIDUAL STRESS

Mechanical behaviour analysis of the proposed switch is performed in COMSOL 5.2 software. Stress analysis is done to understand the stability of the switch during its working at different pull-in voltages. The von mises stress is evaluated to test the defelction of the beam due to stress for the choosen gap. Due to the presence of the dimples, the von mises stress is dispensation around the perforations. During actuation, an electrostatic is generated between beam and lower electrode and is given by [12]–[15].

$$f = \frac{\varepsilon_0 \varepsilon_r S V^2}{2d^2} \tag{7}$$

where,

$\mathcal{E}_r$ is relative permitivity of beam material, S area of the beam in proposed switch,V_p is acuation voltage, d is airgap between signal line and beam.

$$S = A - A_d \tag{8}$$

Force is mainly depends on the area of the beam, airgap between the beam and dielectric material. Residual stress in the beam is related to spring constant because of an beam deflection to the applied voltage is dominated and even existence of minute level in stress. Therefore , force applied on the beam is the key for the low pull-in-voltage.

Different stress analysis are carried out and presented in Table 8 to 12 by using meandering techniques with semi circular disc and vice-versa. Both uniform and non-uniform meanders are observed best results which are enough to handle higher switching to the given maximum stress when compare with other meandering techniques.

D. SWITCHING TIME ANALYSIS

Switching time states that switch is depending on the speed. The formula for switching time anaysis is

$$T_s = \frac{3.67 V_p}{V_s \omega_0} \tag{9}$$

where,

V_s is varying the supply voltage, f_0 is resonant frequency, and V_p is pull-in voltage.

The formula for the angular frequency is

$$\omega_0 = 2\pi f_0 \tag{10}$$

Switching time is directly proportional to actuation voltage and inversely proportional to the supply voltage and angular frequency. In Table 13, presents the simulated value of the resonant frequency with semicircular disc and without disc using different meandering techniques. From Table 13, we have observed that the best switching time analysis is 3.916 μs for two uniform meanders.

E. DAMPING COEFFICIENT AND QUALITY FACTOR

The damping coefficient is helps the beam to return to its original position. The damping of a parallel plate geometries is derived from Reynolds gas-film equation is [16]–[20].

$$b = \frac{3}{2\pi} \frac{\mu (A - A_b)^2}{g_0^3} \tag{11}$$

where,

μ is constant value of $1.885E-5$, $A\text{-}A_b$ is difference between the area of the beam and area of the dimple inserted in switch, g_0 is air gap between the beam and the dielectric layer Damping coefficient is mainly depends on the g_0. In beam the presence of dimples reduces the damping coefficient. The quality factor is used to measure the system energy stored. The quality factor of the beam is determining several different parameters such as intrinsic material dissipation and temperature.

The formula for quality factor is

$$Q = \frac{K_s}{2\pi f_0 b} \tag{12}$$

TABLE 6. Changing the beam thickness of uniform and non-uniform three meanders.

Materials		Three Meanders									
	parameters	Uniform Meanders					Non-uniform meanders				
		1 μm	1.2 μm	1.5 μm	2 μm	3 μm	1 μm	1.2 μm	1.5 μm	2 μm	3 μm
Gold	K_s (N/m)	21.2	36.7	71.92	169.85	573.3	24.9	43.05	84.39	199	672.62
	V_p (V)	10.3	13.5	18.9	29.08	53.45	11.6	15.19	21.27	32.67	60.05
Titanium	K_s (N/m)	31.9	55.1	107.23	254.78	859.9	37.4	64.57	126.16	298.51	1761
	V_p (V)	12.6	16.6	23.14	35.62	65.4	14.15	18.61	26.023	40.01	97.2
Platinum	K_s (N/m)	51	88.1	171.74	407.7	137.85	59.8	103.32	380.95	478.3	2212.12
	V_p (V)	15.9	20.9	29.24	45.1	82.8	17.91	23.54	45	50.6	108.9

TABLE 7. Changing the beam thickness of uniform and non-uniform single meander.

Materials		Single Meander									
	Parameters	Uniform Meanders					Non-uniform meanders				
		1 μm	1.2 μm	1.5 μm	2 μm	3 μm	1 μm	1.2 μm	1.5 μm	2 μm	3 μm
Gold	K_s (N/m)	96.25	163.3	320	756.1	2551.8	129.04	223.5	497.64	1032.4	3485.04
	V_p (V)	36.5	47.6	66.6	102	188.1	46.04	60.6	90.42	130.23	239.3
Titanium	K_s (N/m)	141.7	244.95	478.5	1134.1	3827.8	190.5	334.5	653.3	1548.6	5226.42
	V_p (V)	44.3	58.3	81.4	125.4	230.34	55.9	74.13	103.6	159.5	293
Platinum	K_s (N/m)	227.3	391.8	761.75	1814.6	6124.3	310.1	516.6	1045.3	2476	8362.13
	V_p (V)	56.1	73.7	102.8	158.6	291.35	71.4	92.1	131	201.7	370.64

TABLE 8. Stress analysis by using three unifrom meanders.

parameters	Materials	Gold			Indium			Titanium			Platinum		
	Thickness of the beam (μm)	1.0	1.2	1.5	1.0	1.2	1.5	1.0	1.2	1.5	1.0	1.2	1.5
Stress(MPa)													
(with semi circular disc)		1.89	1.26	0.62	1.89	1.27	0.62	1.92	1.19	0.62	1.9	1.20	0.62
(without semi circular disc)		1.15	0.82	0.57	1.14	0.81	0.57	1.26	0.91	0.61	1.22	0.88	0.59
Total Displacement													
(with semi circular disc)		0.01 E-2	6.9 E-3	3.6 E-3	0.07	0.04 E-2	0.02 E-3	7.1 E-3	4.2 E-3	2.2 E-3	4.9 E-3	2.9 E-3	1.5 E-3
(without semi circular disc)		0.01 E-2	6.6 E-3	3.3 E-3	0.07	0.04 E-7	0.02 E-3	6.6 E-3	4.1 E-3	2.1 E-3	4.5 E-3	2.8 E-3	1.42 E-3
Force		1.9604E-7 N											

TABLE 9. Stress analysis by using three non- unifrom meanders.

parameters	Materials	Gold			Indium			Titanium			Platinum		
	Thickness of the beam (μm)	1.0	1.2	1.5	1.0	1.2	1.5	1.0	1.2	1.5	1.0	1.2	1.5
Stress(MPa)													
(with semi circular disc)		18.4	13.4	12.6	18.4	13.5	12.8	18.1	12.8	10.2	18.2	12.9	11.2
(without semi circular disc)		17.3	12.7	8.58	17.3	12.7	8.57	17.6	12.9	8.75	17.2	12.8	8.69
Total Displacement													
(with semi circular disc)		0.2	0.12	0.07	1.28	0.78	0.44	0.12	0.07	0.04 E-2	0.08	0.05 E-2	0.03 E-2
(without semi circular disc)		0.2	0.12	0.07	1.26	0.75	0.42	0.12	0.07	0.04 E-2	0.08	0.05 E-2	0.03 E-2
Force		2.3089E-6 N											

where, K_s is spring constant, f_0 is resonant frequency and b is damping coefficient. These damping coefficient and quality factor analysis is observed in Table 14.

Here, we have observed that for three uniform and non-uniform meanders $b = 2.966E - 4$, for two meanders $b = 1.682E - 4$ and for single uniform and non-uniform meanders are $b = 3.1622E - 5, 2.72E - 5$ respectively.

TABLE 10. Stress analysis by using double unifrom meanders.

parameters	Materials	Gold			Indium			Titanium			Platinum		
	Thickness of the beam (μm)	1.0	1.2	1.5	1.0	1.2	1.5	1.0	1.2	1.5	1.0	1.2	1.5
Stress(MPa)													
(with semi circular disc)		1.27 E-6	9.38 E-7	6.21 E-7	1.27 E-6	9.26 E-7	6.18 E-7	1.38 E-6	1.04 E-6	6.65 E-7	1.34 E-6	1.02 E-6	6.44 E-7
(without semi circular disc)		1.11 E-6	7.93 E-7	5.33 E-7	1.11 E-6	7.88 E-7	5.29 E-7	1.18 E-6	8.46 E-7	5.8 E-7	1.16 E-6	8.28 E-7	5.64 E-7
Total Displacement													
(with semi circular disc)		1.07 E-8	6.7 E-9	3.7 E-9	6.77 E-8	4.24 E-8	2.35 E-8	6.85 E-9	4.26 E-9	2.34 E-9	4.65 E-9	2.9 E-9	1.59 E-9
(without semi circular disc)		7.74 E-9	4.94 E-9	2.79 E-9	4.9 E-8	3.13 E-8	1.77 E-8	4.86 E-9	3.07 E-9	1.72 E-9	3.32 E-9	2.11 E-9	1.18 E-9
Force		4.967576E-5 N											

TABLE 11. Stress analysis by using single unifrom meander.

parameters	Materials	Gold			Indium			Titanium			Platinum		
	Thickness of the beam (μm)	1.0	1.2	1.5	1.0	1.2	1.5	1.0	1.2	1.5	1.0	1.2	1.5
Stress(MPa)													
(with semi circular disc)		1.67 E-3	390	250	2.31E3	386	248	2.51E3	416	269	2.44E3	411	265
(without semi circular disc)		575	318	211	572	316	211	630	338	215	604	331	209
Total Displacement													
(with semi circular disc)		4.32	2.86	1.44	27.4	18.1	9.12	2.95	1.87	0.94	1.96	1.25	0.63
(without semi circular disc)		3.2	1.98	0.96	20.3	12.5	6.02	2.05	1.24	0.6	1.39	0.85	0.41
Force		1.44282E-4 N											

TABLE 12. Stress analysis by using single non unifrom meander.

parameters	Materials	Gold			Indium			Titanium			Platinum		
	Thickness of the beam (μm)	1.0	1.2	1.5	1.0	1.2	1.5	1.0	1.2	1.5	1.0	1.2	1.5
Stress(MPa)													
(with semi circular disc)		1.78E3	326	209	1.77E3	323	207	1.9E3	379	232	1.84E3	362	223
(without semi circular disc)		454	247	179	451	245	179	496	267	175	475	259	174
Total Displacement													
(with semi circular disc)		3.32	2.09	1.1	21	13.2	6.98	2.21	1.37	0.72	1.47	0.92	0.48
(without semi circular disc)		2.39	1.47	0.81	15.1	9.33	5.12	1.52	0.93	0.51	1.03	0.63	0.34
Force		1.187055E-4 N											

TABLE 13. Switching time analysis using uniform and non uniform meanders.

Parameters	Three meanders		Two meanders	Single meanders	
	Uniform	Non-uniform	Uniform	Uniform	Non-uniform
Resonant frequency(f_0)					
(with semicircular disc)	1.113E5	94037	1.3684E5	1.5224E5	1.133E5
(without semicircular disc)	1.1955E5	95937	1.6131E5	1.96043E5	1.408E5
Switching time (t_s)					
(with semicircular disc)	5.41 μs	3.939 μs	3.91617 μs	4.5055 μs	5.1184 μs
(without semicircular disc)	5.035 μs	3.29 μs	3.126 μs	4.4163 μs	4.15567 μs

F. EFFECT OF DAMPING AND QUALITY FACTOR IN RELEASE TINE

Damping coefficient is inversely proportional to the quality factor. This quality factor will have great influence in switching and release times. The range of the quality is given as 0.5 – 2 such that switches with quality factor less than 0.5 will suffers fast switching and if greater than 2 will suffers from low release times and quality factor is approximately

TABLE 14. Varying the values of damping coefficient and quality factor using different meanders.

Parameters & Materials	Air gap (μm)	Three Meanders								Single Meander							
		Uniform				Non-uniform				Uniform				Non-uniform			
		0.9	1	1.2	1.5	0.9	1	1.2	1.5	0.9	1	1.2	1.5	0.9	1	1.2	1.5
Damping Coefficient (b)		2.97 E-4	2.16 E-4	1.25 E-4	6.41 E-5	2.55 E-4	1.86 E-4	1.08 E-4	5.52 E-5	3.16 E-5	2.78 E-5	1.61 E-5	8.25 E-6	2.72 E-5	1.98 E-5	1.15 E-5	5.87 E-6
Quality factor(q)																	
Gold (with semicircular disc)		0.10 2	0.14	0.18	0.23	0.17	0.22	0.39	0.76	3.18	3.62	6.25	12.2	6.66	9.14	15.8	30.9
(without semicircular disc)		0.01	0.13	0.16	0.21	0.16	0.23	0.38	0.75	2.55	2.89	5.01	9.75	5.4	7.36	12.7	24.8
Titanium (with semicircular disc)		0.06	0.09	0.12	0.14	0.1	0.13	0.22	0.43	1.63	1.85	3.20	6.25	2.21	3.03	5.24	10.2
(without semicircular disc)		0.06	0.08	0.10	0.13	0.1	0.12	0.21	0.42	1.27	1.44	2.5	4.87	1.66	2.27	3.92	14.5
Platinum (with semicircular disc)		0.18	0.25	0.29	0.40	0.27	0.37	0.64	1.25	4.64	5.3	9.1	17.8	6.5	8.89	15.4	30.1
(without semicircular disc)		0.17	0.24	0.28	0.38	0.33	0.36	0.62	1.22	3.7	4.16	7.2	14.0	4.6	6.64	14.5	22.2

"1" is recommended for the best release response. The formula for settling time which is related to quality factor is [21]–[23].

$$t_s = \frac{27V_p^2}{4\omega Q V_s^2} = \frac{2bV_P^2}{g_0 V_s^2} \tag{13}$$

where,

t_s is the overestimate the switching time ,V_p is pull-in-voltage, ω_0 is angular frequency, Q is the quality factor, V_s is supply voltage, b is damping coefficient, g_0 is air gap between the beam and the dielectric layer.

G. CAPACITIVE ANALYSIS OF A SWITCH

RF MEMS Switch can develop the capacitance in terms of up state and down state.

Formula for the up-state capacitance is [6], [24]–[26].

$$C_u = \frac{\varepsilon_0(A - A_d)}{g_0 + \frac{t_d}{\varepsilon_r}} \tag{14}$$

where,

C_u is upstate capacitance, ε_r is relative Permittivity of a dielectric material, t_d is the thickness of the dielectric layer, $A\text{-}A_d$ is difference between the area of the beam and area of the dimple is inserted in switch, $\mathcal{E}_0$ is permittivity of free space and $g_0$is air gap of the given switch. Based on the relative permittivity of the dielectric material the variation in capacitance occurs. The various dielectric materials are considered to analyze the charging and discharging of switch.

The down state capacitance is

$$C_d = \frac{\varepsilon_0\varepsilon_r\,(A - A_d)}{t_d} \tag{15}$$

The capacitance ratio states that the ratio between down state to upstate capacitance. This capacitance ratio is depends on the efficiency of a switch. Then the formula for the capacitance ratio is

$$C_r = \frac{C_d}{C_u} = \frac{\frac{\varepsilon_r\varepsilon_0(A-A_d)}{t_d}}{\frac{\varepsilon_0(A-A_d)}{g_0+\frac{t_d}{\varepsilon_r}}} \tag{16}$$

where,

C_u is up state capacitance, C_d is down state capacitance and C_r is the Capacitance ratio and it is mainly depending on the relative permittivity, thickness and area of the beam. Upstate capacitance is based on both insertion and isolation losses and down state capacitance is based on the isolation. Capacitance is depending on dielectric material, dielectric thickness and beam materials.

The different beam materials have been used to determine the capacitance ratio of the proposed RF MEMS switch which decreases the losses. Gold material having relative permitivity 6.9 is chosen as beam material and capacitance ratio of 7.12, 6.17 and 5.14 is obtained for beam thickness of 1μm, 1.2μm and 1.5μm respectively whereas by varying the denominator of the Cr which is known as upstate capacitance, it can be observed as 7.12, 7.9, 9.28, 11.35 for the air gap between the dielectric layer and the beam with 0.9 μm, 1 μm, 1.2 μm and 1.5 μm respectively. These capacitance

TABLE 15. Varying thickness using uniform and non-uniform meanders.

Parameters	Three Meanders						Single Meander					
	Uniform			Non-Uniform			Uniform			Non-Uniform		
Thickness (μm)	1	1.2	1.5	1	1.2	1.5	1	1.2	1.5	1	1.2	1.5
Down state Capacitance (C_d) Units:(pico Farads(pF))	0.299	0.25	0.20	0.2774	0.232	0.185	0.108	0.0896	0.072	0.091	0.076	0.061
Upstate Capacitance(C_u) Units:(femito Farads(fF))	41.5	40.5	38.8	38.6	37.52	36.1	14.9	14.5	13.9	12.6	12.2	11.8
Capacitance ratio (C_r)	7.12	6.17	5.14	7.21	6.2	3.29	7.21	6.17	5.14	7.21	6.18	5.14

TABLE 16. Varying airgap using uniform and non-uniform meanders.

Parameters	Three Meanders								Single Meander							
	Uniform				Non-Uniform				Uniform				Non-Uniform			
Airgap (μm)	0.9	1	1.2	1.5	0.9	1	1.2	1.5	0.9	1	1.2	1.5	0.9	1	1.2	1.5
Downstate Capacitance (C_d) Units:(pico Farads(pF))	0.2994				0.2780				0.1075				0.907			
Upstate Capacitance(C_u) Units:(femito Farads(fF))	41.5	37.9	32.7	26.4	38.6	35.2	30.1	24.5	14.9	13.6	11.6	9.47	12.6	11.5	9.8	7.99
Capacitance ratio (C_r)	7.12	7.9	9.28	11.4	7.21	7.9	9.3	11.4	7.21	7.9	9.3	11.4	7.21	7.9	9.3	11.4

analyses are done with different materials in Table 15 and Table 16 respectively.

IV. RESULTS AND DISCUSSIONS

The proposed RF MEMS capacitive shunt switch is performed with different analysis such as electromechanical analysis, stress, switching time and electromagnetic analysis. By these analysis, it is clear that the best material and suitable dimensions are choosen for fabrication.

A. ELECTROMECHANICAL ANALYSIS

1) UNIFORM THREE MEANDERS

The proposed switch for uniform 3 meanders is designed and simulated by FEM tool and analysed by changing beam thickness, beam material, air gap and changing the substrate, dielectric and airgap etc.

The simulations are carried out with and without semi-circular disc as shown in Figure 4 & 5. The semicircular disc is used to reduce the residual stress and the voltage versus displacement analysis are done by using different beam materials such that gold, platinum and titanium are shown in Figure.6. Here, we have observed that platinum shows better results than gold but it is costlier than gold. Hence gold is chosen as the best material to enhance the switch characteristics. In figure 7, the dispalcement of the beam by actuation voltage for dfferent airgaps such as 0.9 μm, 1 μm, 1.2 μm and 1.5 μm and it is observed that 0.9μm gap shows better displacement having slope nearly 1. In figure 8, it can be observe that 1 μm thickness shows as a good displacement when compare with the 1.2 μm and 1.5 μm beam thickness.

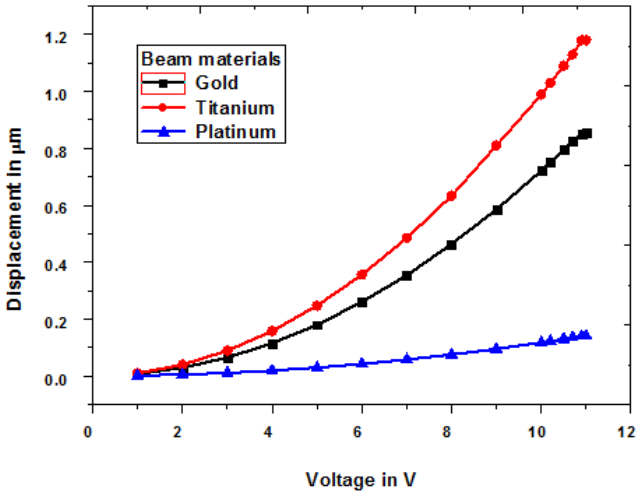

FIGURE 6. Voltage versus displacement using three unifrom meanders for different beam materials.

2) UNIFORM TWO MEANDERS

The proposed switch is implementing with uniform two meanders without changing the movable beam dimensions. The analysis are done by using different beam thickness, beam materials and airgap between the signal line and the beam and are presented in Figures from 9 to 13.

The Figure 11 and 12 illustrates the impact of semi circular disc which increases the stability of the switch during the displacement. The switch without disc shows the displacement which is greater than the gap taken.

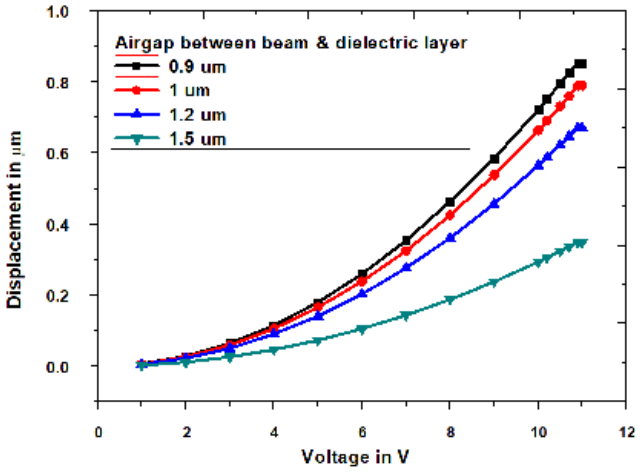

FIGURE 7. Voltage versus displacement using three unifrom meanders for different airgaps.

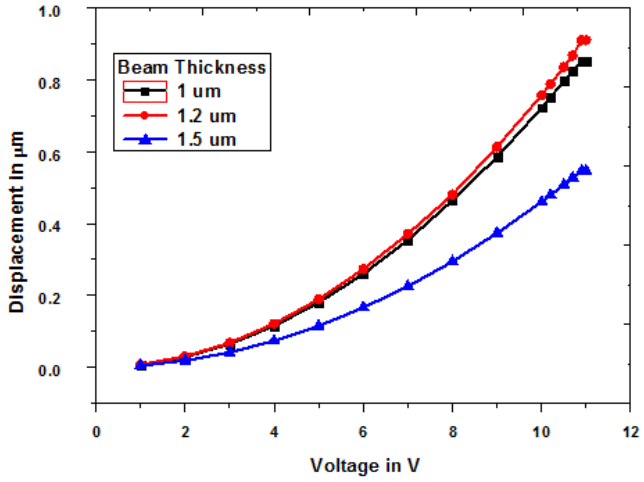

FIGURE 8. Voltage versus displacement using three unifrom meandersfor different beam thickness.

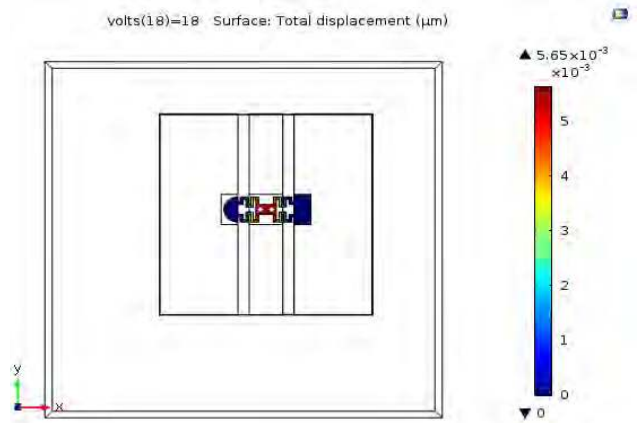

FIGURE 9. Voltage versus displacement of a proposed switch with semi circular disc using two uniform meanders.

The semicircular disc increases the stifness by firm holding the meanders gives the displacement with in the range of gap taken.

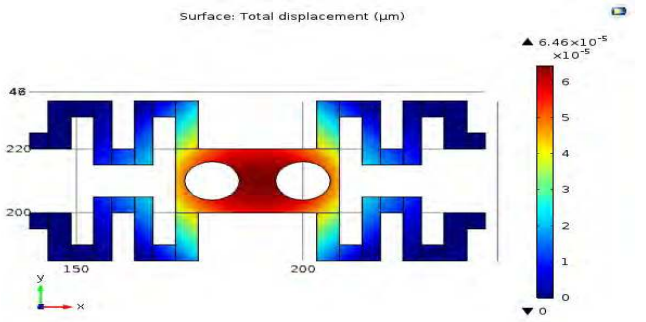

FIGURE 10. Voltage versus displacement a proposed switch without semi circular disc using two uniform meanders.

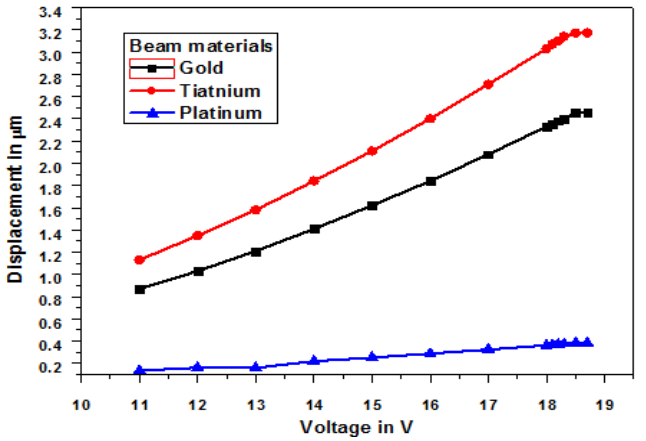

FIGURE 11. Voltage versus displacement using two meanders for different beam Materials.

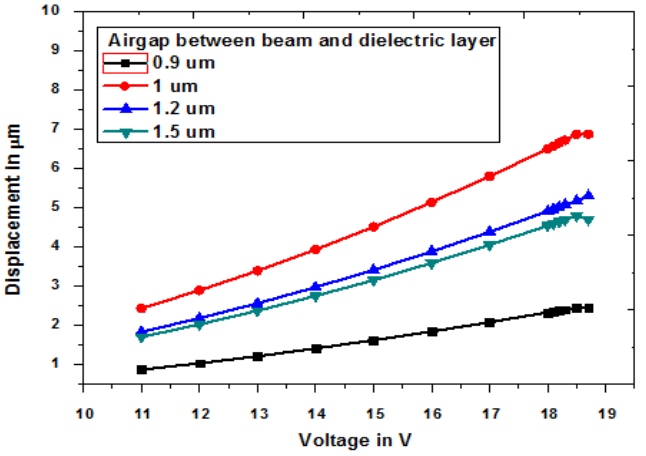

FIGURE 12. Voltage versus displacement using two meanders for different airgap.

The switch with beam thickness 1.2 μm having the air gap of 0.9 μm with the gold material is observed as the suitable parameters for better performance of switch with two meanders.

3) UNIFORM SINGLE MEANDER

The proposed switch is designed using single meander with uniform structure and the observations are discussed from the Figure 14 to Figure 18.

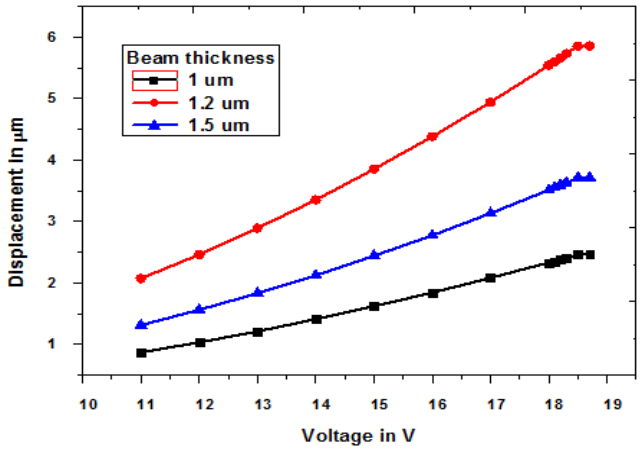

FIGURE 13. Voltage versus displacement using two meanders for different thickness.

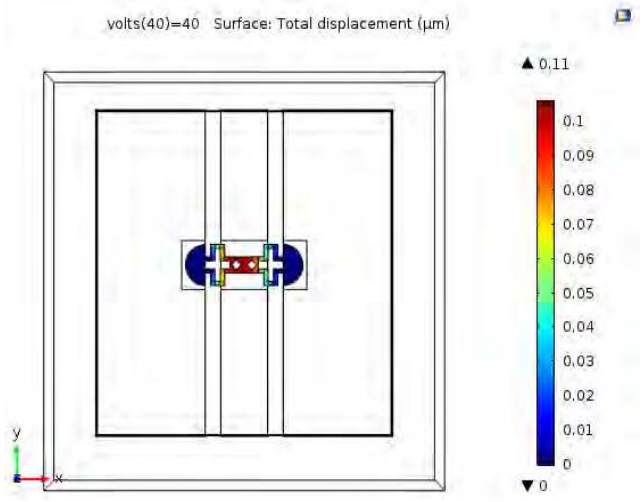

FIGURE 14. Voltage versus displacement of a switch with semi circular disc using single uniform meander.

The switch with single meander is analyzed by taking semi circular discs and observed that beam displaces the gap at pull-in voltage and it shows the displacement out of range when discs are not considered. Hence the discs are also plays a major role in uniform single meander.

The uniform one meander switch is analysed by varying the gap, thickness and material as shown in the Figures from 14 –18. The switch shows better performance with the parameters at 0.9 μm air gap with 1μm beam thickness made up of gold material.

4) NON-UNIFORM THREE MEANDERS

The proposed switch with non-uniform three meanders is used instead of uniform three meanders. By comparing this analysis for both uniform and non-uniform three meanders, it is observed that the non-uniform three meanders shows better results. This analysis is observed in Figure 19-23.

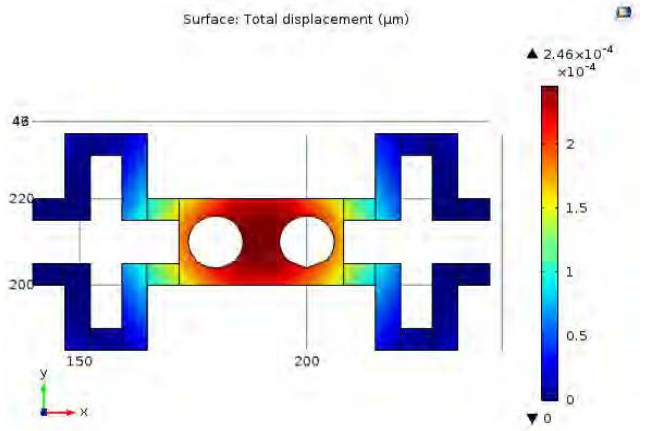

FIGURE 15. Voltage versus displacement of a switch with out semicircular disc using single uniform meander.

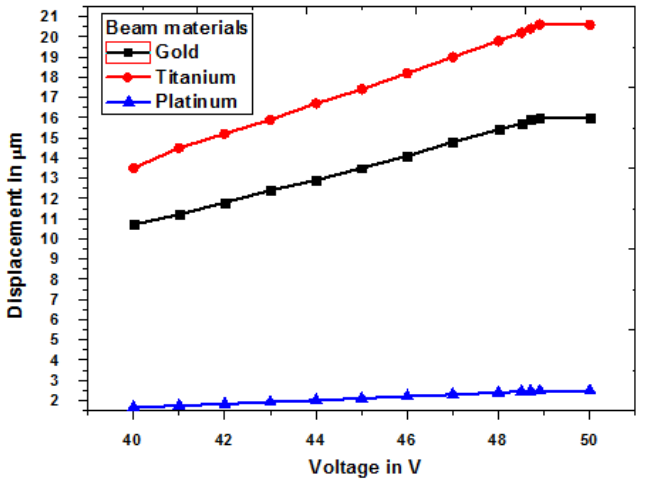

FIGURE 16. Voltage versus displacement using single uniform meander for different beam material.

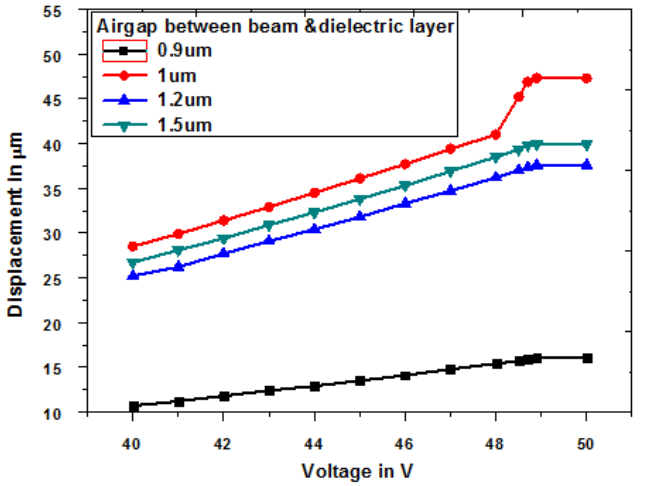

FIGURE 17. Voltage versus displacement using Single uniform meander for different airgaps.

The switch designed with non-uniform three meanders is analyzed from Figure 19 to 23 and it observed that the proposed meanders also shows good performance at 0.9 μm with platinum as a beam material having thickness 1 μm.

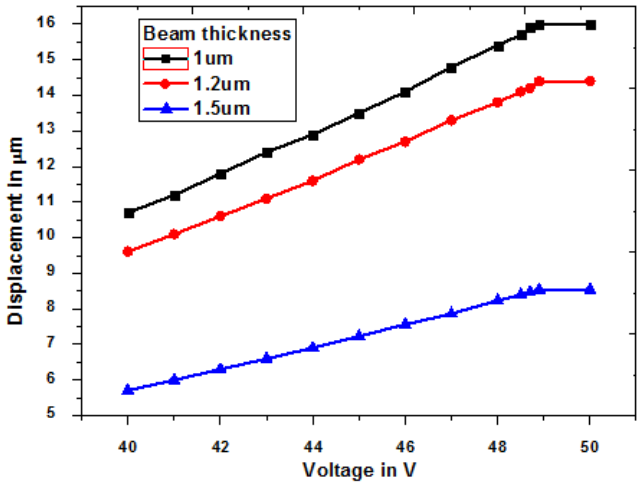

FIGURE 18. Voltage versus displacemnt using single uniform meander for different thickness.

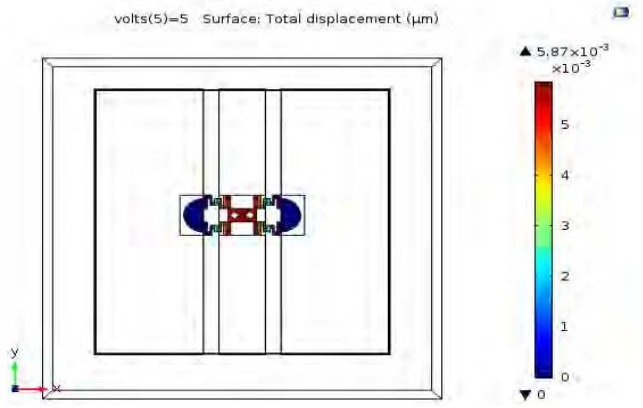

FIGURE 19. Voltage versus displacement of a proposed switch with semicircular disc using non- uniform three meanders.

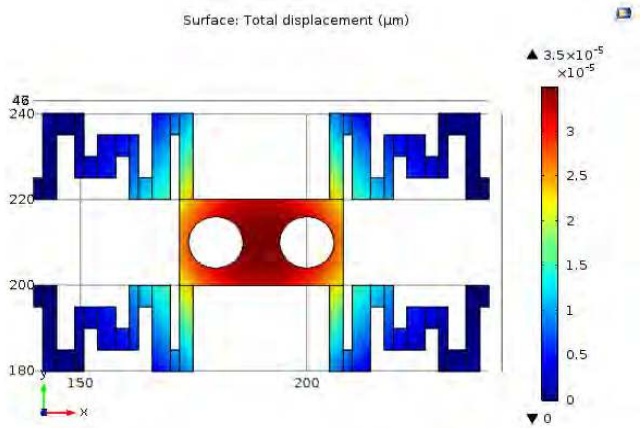

FIGURE 20. Voltage Versus displacementr a Switch without semi circular disc using Non uniform three Meanders.

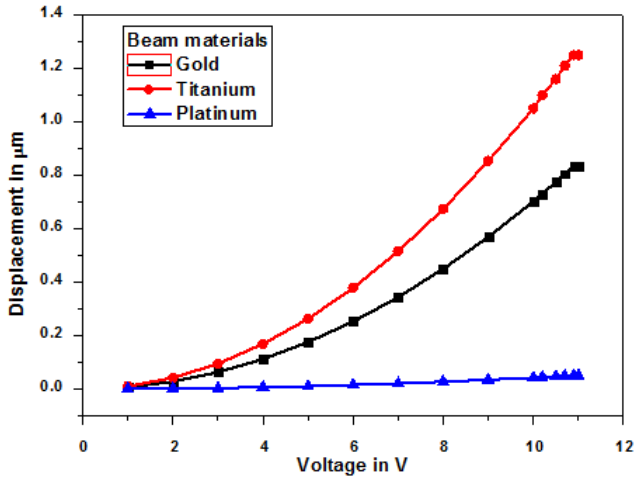

FIGURE 21. Voltage versus displacement using non -uniform three meanders for different beam material.

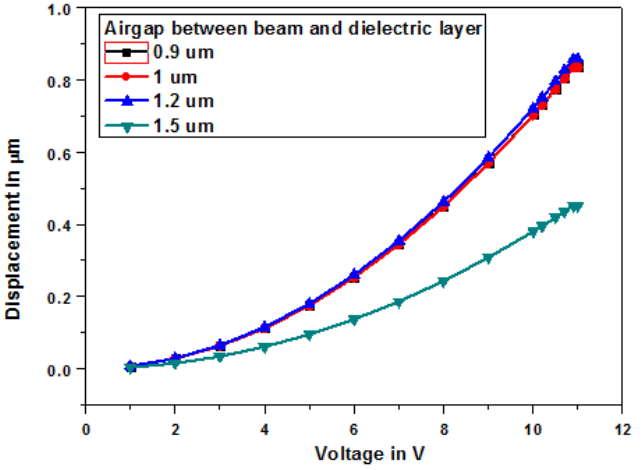

FIGURE 22. Voltage versus displacement using non -uniform three meanders for different airgaps.

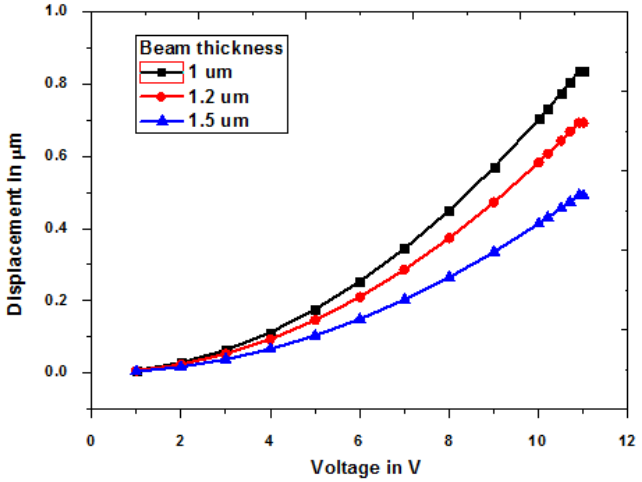

FIGURE 23. Voltage versus displacement using non -uniform three meanders for different thickness.

5) NON-UNIFORM SINGLE MEANDER

The proposed switch is implemented with non- uniform single meander instead of uniform single meanders. When compare with all uniform meanders and non-uniform three meanders, the non-uniform single meander exhibits good results. This analysis is observed in Figure 24-28.

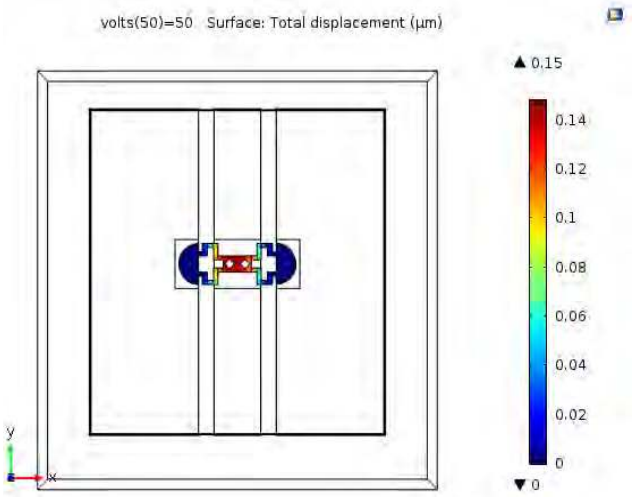

FIGURE 24. Voltage versus displacement of a proposed switch with semicircular disc using non- uniform single meander.

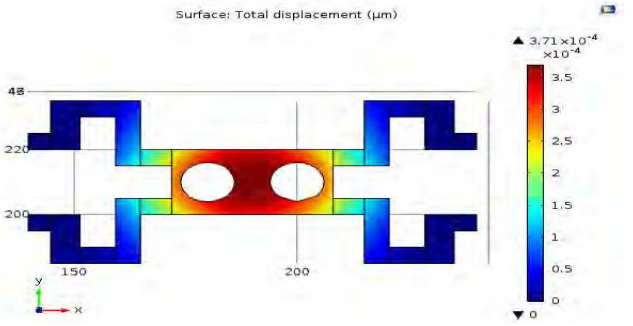

FIGURE 25. Voltage versus displacement of a proposed switch without semicircular disc using non-uniform single meander.

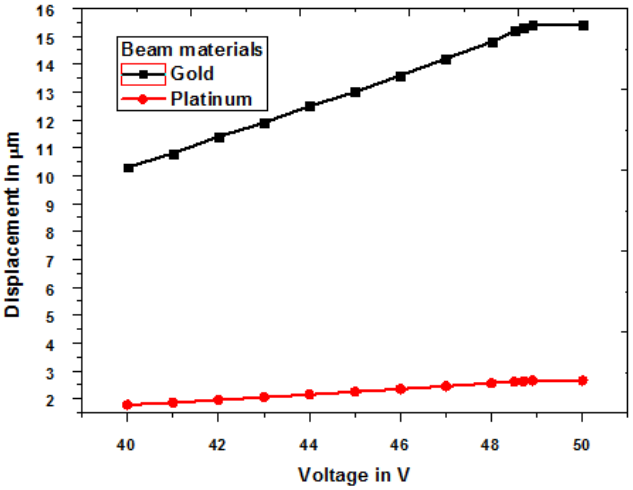

FIGURE 26. Voltage versus displacement using non- uniform single meander for different beam material.

6) COMPARISION BETWEEN BOTH UNIFORM AND NON-UNIFORM MEANDERS

Electromechanical analysis has done with voltage versus displacement comparison by using both uniform and

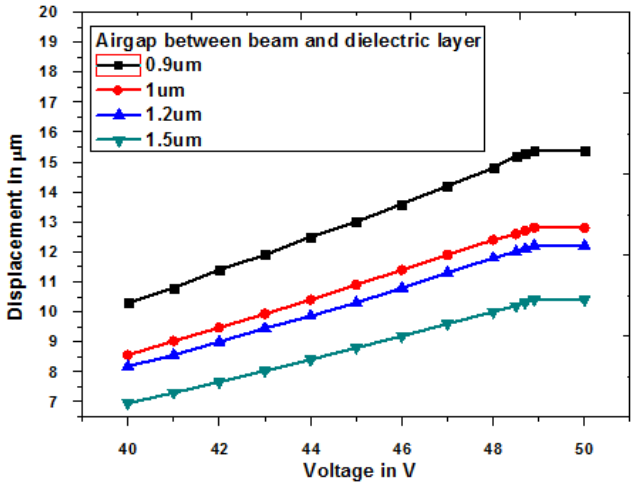

FIGURE 27. Voltage versus displacement using non -uniform single meander for different airgaps.

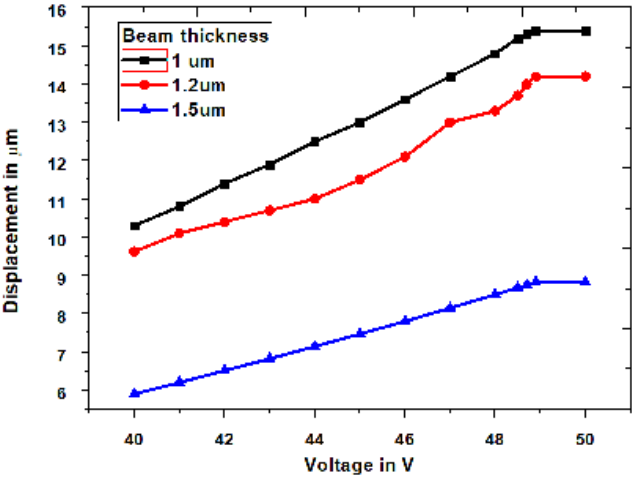

FIGURE 28. Voltage versus displacement using non- uniform single meander for different thickness.

non-uniform three, single meanders. Here we observed three uniform meanders as better results when compare with three non-uniform meanders in Fig 29.

The comparison between uniform and non-uniform meanders are shown in Figure 29 observes proper results in non-uniform three meanders when compare with uniform meanders. Similar analysis done in Figure 30 using uniform and non-uniform single meander. In figure 30, we observes single uniform meander is better when compare with single non-uniform meander.

B. STRESS ANALYSIS

The stress analysis has been carried out by considering the different beam materials and thickness of beam.

The stress analyses are carried out with uniform load and it is observed that switch can withstand by having stress 1.9 MPa by using semi-circular disc as shown in

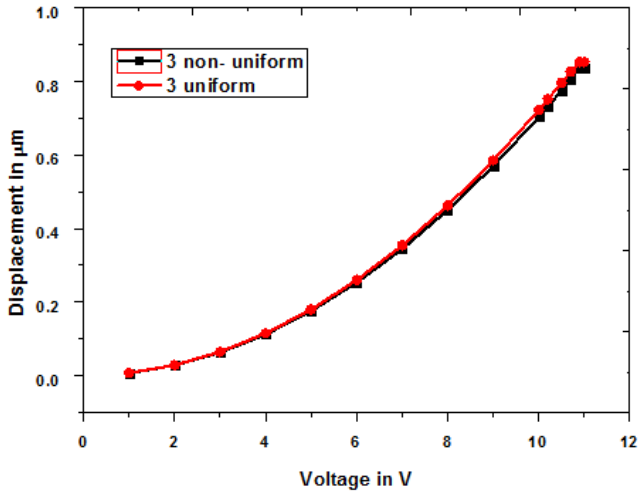

FIGURE 29. Voltage versus displacement of both uniform and non- uniform three meanders.

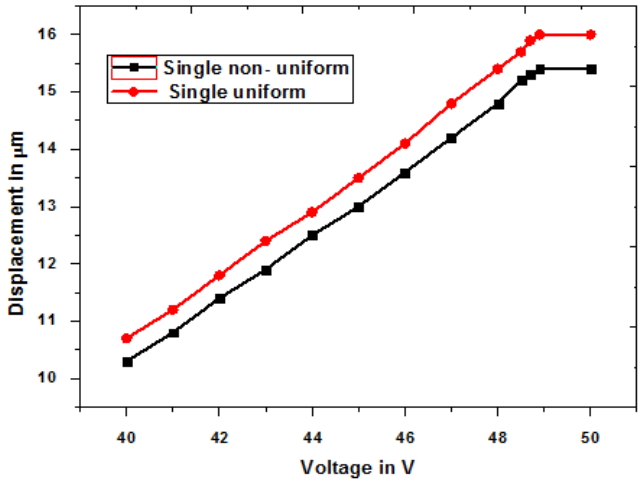

FIGURE 30. Voltage versus displacement of both non- uniform and uniform single meander.

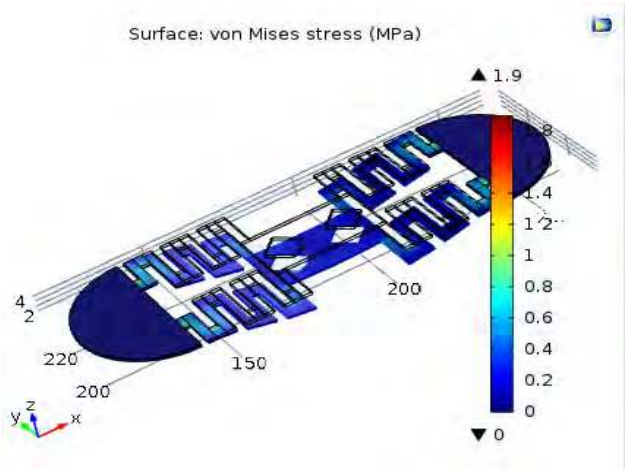

FIGURE 31. A switch having semicircular disc by using three uniform meanders for a gold material at 1μm thickness.

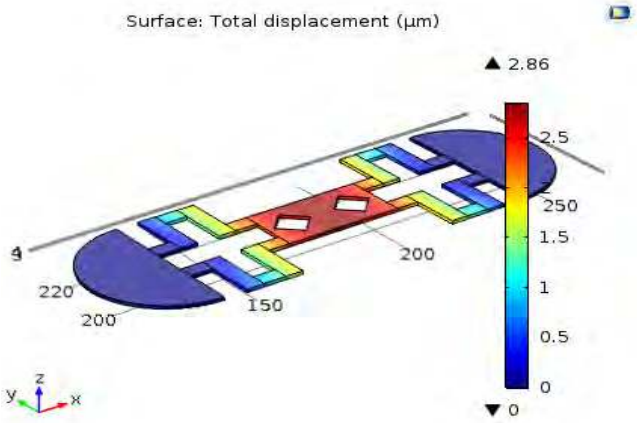

FIGURE 32. Total displacement having with semicircular disc using single uniform meanders for a gold Material at 1.2 μm thickness.

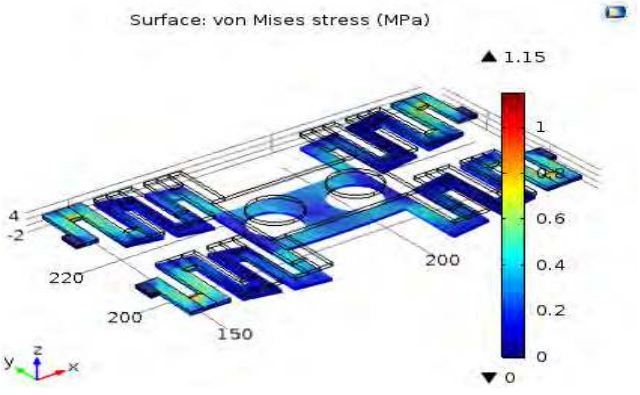

FIGURE 33. A Switch having without semicircular disc by using three uniform meanders for a gold as a beam material.

the Figure 31. The switch without the disc can withstand upto 1.15 MPa which is lower in the case of using disc.

C. SWITCHING TIME ANALYSIS

The switching time analysis have been carried out for uniform and uniform meander and the values are presented in the Table 12. Among the non-uniform meanders, the switch having three meanders takes very less time of 3.9 μsec for switching and uniform two meanders show 3.126 μsec. The low switching time of the proposed switches shows the fast transition of the switch from ON state to OFF state and the calibration of the switch is presented in the Figure 35 and 36.

D. DAMPING COEFFICIENT AND QUALITY FACTOR RELATED TO SETTLING TIME

The relation between time, quality factor and damping coefficient has shown in the equation 13. The settling time for different meandering techniques is performed and presented in the Figure 37. It shows the uniform and non–uniform single meander shows very less releasing time with low damping effect.

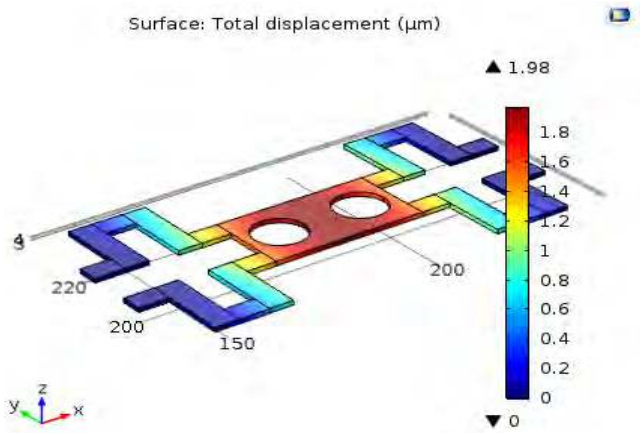

FIGURE 34. Total displacement having without semicircular disc using three uniform meanders for a gold as a beam Material.

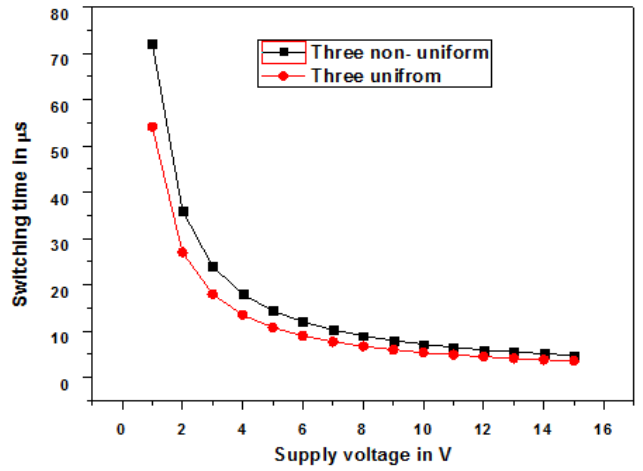

FIGURE 35. Voltage versus switching time analysis using both uniform and non-uniform three meanders.

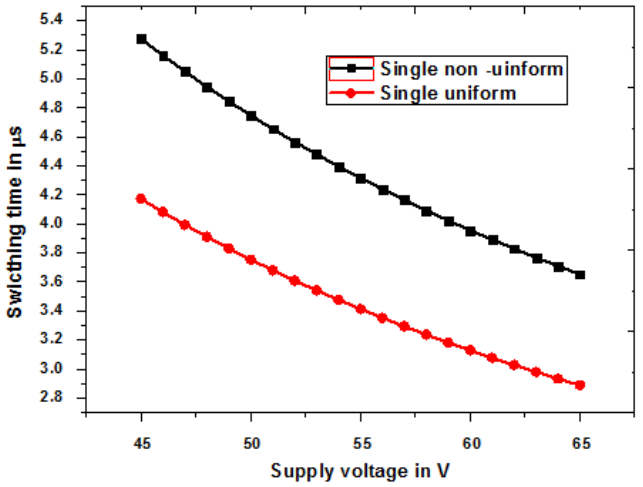

FIGURE 36. Voltage versus switching time analysis using both single uniform and non-uniform meanders.

E. CAPACITANCE ANALYSIS OF A SWICTH

The capacitance developed between the beam and lower electrode is used to regulate the transmission of RF signal.

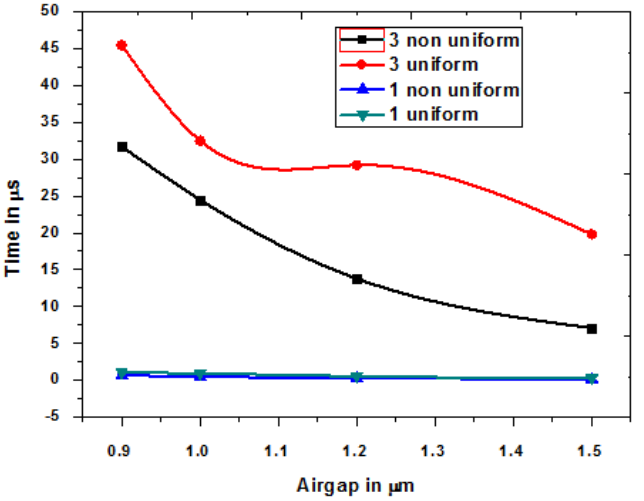

FIGURE 37. Time versus gap in damping-limited case.

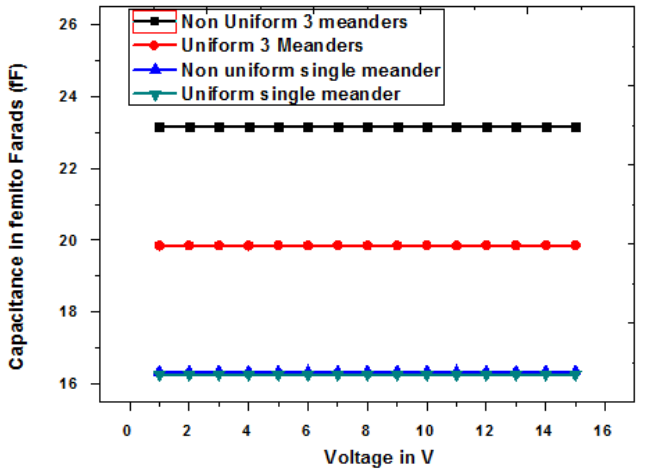

FIGURE 38. Capacitance versus voltage of all meandering techniques.

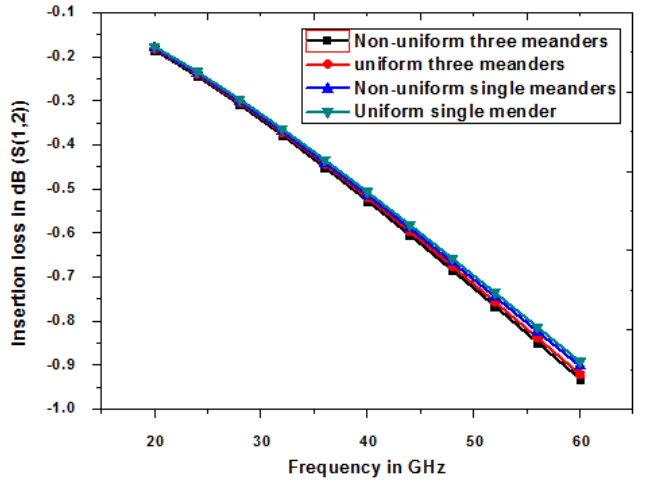

FIGURE 39. Insertion loss of a frequency at 40 GHz by using all meandering techniques.

From the Figure 38 we observed that 23 fF (femito Farads) of capacitance is developed for non-uniform three meanders which is higher than the other type of switches in upstate capacitance condition.

TABLE 17. Comparision between uniform and non uniform 3 meanders and single meander.

Parameters (40 GHz frequency)	Three Meanders		Single Meander	
	Unifrom	Non-uniform	Uniform	Non-uniform
Isolation	-36.37 dB	-39.973 dB	-44.64 dB	-54.171 dB
Return loss	-16.37 dB	-16.06 dB	-17.61 dB	-17.35 dB
Insertion loss	-0.52 dB	-0.52 dB	-0.51 dB	-0.514 dB

F. RF PERFORMANCE ANALYSIS

Electromagnetic analysis is done using HFSS. In these proposed switches, to analyse the performance, scattering parameters such as isolation, insertion and return loss are used for different uniform and non-uniform meandering techniques. This RF properties are analysed over the 26.5 GHz to 40 GHz frequency range. When comparing with all meandering techniques we observed good results in return loss for uniform single meander as −17.65 dB, low Insertion loss for uniform single meander as −0.51 dB and high isolation for non-uniform single mender as −54.18 dB.

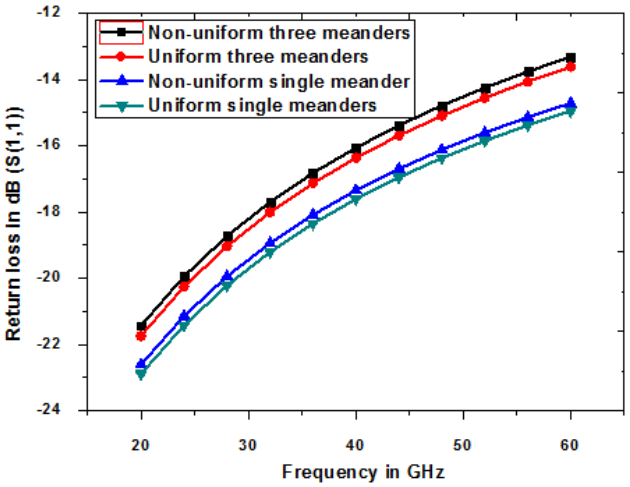

FIGURE 40. Return loss of a frequency at 40 GHz by using all meandering techniques.

This RF analysis are mainly depends on the dielectric material and thickness of the beam. The analysis presented in table 18 and table 19 are having different dielectric materials and different thickness. Finally, the proposed switches are

TABLE 18. Comparison between uniform and non uniform three meanders.

Parameters (40 GHz frequency)	Dielectric thickness	Three Meanders (3μm Beam thickness)					
		Uniform meanders			Non-unifrom meanders		
		0.1 μm	0.05 μm	0.01 μm	0.1 μm	0.05 μm	0.01 μm
Isolation		-20.6139 dB	-28.4824 dB	-36.37 dB	-20.224 dB	-27.0086 dB	-39.973 dB
Return loss		-20.372 dB	-20.6616 dB	-20.889 dB	-20.109 dB	-20.4394 dB	-20.612 dB
Insertion loss		-0.4307 dB	-0.4273 dB	-0.4266 dB	-0.4281 dB	-0.4259 dB	-0.4242 dB

TABLE 19. Comparison between uniform and non uniform single meander.

Parameters (40 GHz frequency)	Dielectric thickness	Single Meander (3μm Beam thickness)					
		uniform meanders			non-unifrom meanders		
		0.1 μm	0.05 μm	0.01 μm	0.1 μm	0.05 μm	0.01 μm
Isolation		-17.4599 dB	-24.372 dB	-44.6355 dB	-17.074 dB	-23.78 dB	-54.1771 dB
Return loss		-20.6192 dB	-20.897 dB	-21.188 dB	-20.385 dB	-20.74 dB	-21.0724 dB
Insertion loss		-0.4396 dB	-0.4365 dB	-0.4339 dB	-0.4436 dB	-0.4375 dB	-0.4355 dB

TABLE 20. Comparison of proposed capacitive rf mems shunt switch at 1 to 40 ghz with previous works.

Parameters	References			
	Reference [2]	Reference [7]	Reference [8]	Proposed switch
Meandering techniques	-----	-----	-----	Both uniform and non-uniform meanders
Actuation Mechanism	Electromagnetic analysis	Electromechanical and Electromagnetic analysis	Electromagnetic analysis	Electromechanical and Electromagnetic analysis
Substrate Material	GaAs	-----	-----	Quartz
Bridge thickness and material	Gold(2 μm)	1 μm	1 μm	Gold (μm)
Airgap	2 μm	1.2-1.6 μm	3 μm	1 μm and 3 μm
Dielectric thickness and material	0.15μm(Si3N4)	1000 μm	0.3 μm	0.1 μm (ALN)
Pull-in-Voltage	-----	18 and 25 V	18 V	10.3 V
Stress analysis	-----	15 and 25 (MPa)	-----	1.78E3 (MPa) (Gold)
Switching time	-----	3.5 μs	-----	3.126 μs
Isolation	-48 dB	-18 dB	-29 dB	-54.17 dB
Insertion loss	-0.34 dB	-0.9 dB	-0.92 dB	-0.4355 dB
Return loss	-17 dB	-24 dB	-12 dB	-21.072 dB

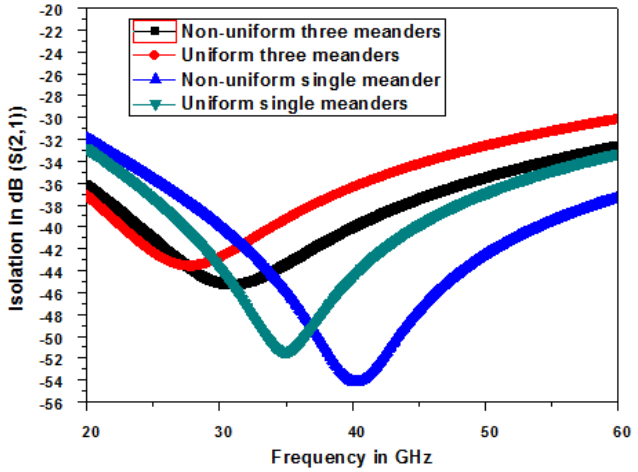

FIGURE 41. **Isolation of a frequency at 40 GHz by using all meandering techniques.**

comparing with both uniform and non-uniform meandering techniques compared and observed excellent RF performances in non-uniform single meander and it is highly recommended to fabricate a proposed switch.

V. CONCLUSIONS

In this paper, the design, analysis and simulation of the proposed RF MEMS shunt switch is done using different meanders along with dimples. Using electromechanical study, pull-in voltage, capacitance ratio, switching time, stress analysis is carried out. Similarly, with the help of electromagnetic study RF losses have been studied. Different materials such as gold, titanium, platinum and indium are chosen for the beam to obtain best performance. Among those above given materials gold is suited as best because of its high conductivity properties. Pull-in-voltage is obtained as 10.3 V for three uniform meanders which is having lower actuation voltage. The switching time of two uniform meander switch is 3.126 μs. The capacitance analysis of a three uniform meanders switch is having up state capacitance as 41.5 fF, down state capacitance as 0.299 pF and capacitance ratio as 7.12 in 1 μm beam thickness. Scattering parameters of the proposed switches are isolation, insertion loss and return loss. The Insertion loss obtained less than -0.514 dB, return loss as -17.34 dB over 1-40 GHz frequency and high isolation observed as -54.17 dB. Compare with other meandering techniques non-uniform meander is produce better performance and it is highly recommended to fabricate the proposed RF MEMS switch for millimetre wave satellite communications and 5G communication at 40 GHz frequency.

ACKNOWLDEGMENT

The authors would like to thank NMDC, supported by Govt. of India, for providing necessary design facilities through NPMASS.

REFERENCES

[1] S. Shekhar, K. J. Vinoy, and G. K. Ananthasuresh, "Low-voltage high-reliability MEMS switch for millimetre wave 5G applications," *J. Micromech. Micro Eng.*, vol. 28, no. 7, pp. 1–15, Aug. 2018.

[2] D. R. Shah, R. Sharma, and H. K. Varshney, "Study of RF-MEMS capacitive shunt switch for microwave backhaul applications," *J. Electron. Commun. Eng.*, vol. 12, no. 1, pp. 57–65, 2017.

[3] S. Shekhar, K. J. Vinoy, and G. K. Ananthasuresh, "Design, fabrication and characterization of capacitive RF MEMS switches with low pull-in voltage," n *Proc. IEEE Int. Microw. RF Conf. (IMaRC)*, Dec. 2014, pp. 182–185.

[4] D. Z. Milosavljevic, "RF MEMS Switches," *Mikrotalasna Revija*, vol. 10, no. 1, pp. 2–8, 2004.

[5] K. S. Rao *et al.*, "Design and simulation of fixed-fixed flexure type RF MEMS switch for reconfigurable antenna," *Microsyst. Technol.*, vol. 15, pp. 1–8, Aug. 2018.

[6] H. R. Ansari and S. Khosroabadi, "Design and simulation of a novel RF MEMS shunt capacitive switch with a unique spring for Ka-band application," *Microsyst. Technol.*, vol. 5, pp. 1–10, Jul. 2018.

[7] Y. Mafinejad, A. Kouzani, K. Mafinezhad, and R. Hosseinnezhad, "Low insertion loss and high isolation capacitive RF MEMS switch with low pull-in voltage," *Int. J. Adv. Manuf. Technol.*, vol. 93, nos. 1–4, pp. 661–670, Aug. 2017.

[8] L. Muhua, J. Zhao, Z. You, and G. Zhao, "Design and experimental validation of a restoring force enhanced RF MEMS capacitive switch with Stiction-recovery electrodes," *Microsyst. Technol.*, vol. 23, no. 8, pp. 3091–3096, Aug. 2017.

[9] M. B. Subramanian, C. Joshitha, B. S. Sreeja, and P. Nair, "Multiport RF MEMS switch for satellite payload applications," *Microsyst. Technol.*, vol. 24, no. 5, pp. 2379–2387, May 2018.

[10] K. S. Rao, L. N. Thalluri, K. Guha, and K. G. Sravani, "Fabrication and characterization of capacitive RF MEMS perforated switch," *IEEE Access*, vol. 6, pp. 77519–77529, 2018. doi: 10.1109/ACCESS.2018.2883353.

[11] K. G. Sravani, T. L. Narayana, K. Guha, and K. S. Rao, "Role of dielectric layer and beam membrane in improving the performance of capacitive RF MEMS switches for Ka-band applications," *Microsyst. Technol.*, vol. 5, pp. 1–10, Aug. 2018. doi 10.1007/s00542-018-4038-4.

[12] Z. Deng, X. Guo, H. Wei, J. Gan, and Y. Wang, "Design, Analysis, and Verification of Ka-BandPattern Reconfigurable Patch Antenna Using RF MEMS Switches," *Micromachines*, vol. 7, p. 144, Aug. 2016.

[13] L.-Y. Ma, N. Soina, and A. N. Nordin, "A K-band switched-line phase shifter using novel low-voltage low-loss RF-MEMS switch," in *Proc. IEEE Regional Symp. Micro Nanoelectron. (RSM)*, Aug. 2017, pp. 14–17.

[14] H. Jaafar, K. S. Beh, N. A. M. Yunus, W. Z. W. Hasan, S. Shafie, and O. Sidek, "A comprehensive study on RF MEMS switch," *Microsyst. Technol*, vol. 20, no. 2, pp. 2109–2121, Dec. 2014.

[15] S. Molaei and B. A. Ganji, "Design and simulation of a novel RF MEMS shunt capacitive switch with low actuation voltage and high isolation," *Microsyst. Technol*, vol. 23, no. 6, pp. 1907–1912, Jun. 2017.

[16] A. K. Ravirala, L. K. Bethapudi, J. Kommareddy, B. S. Thommandru, and S. Jasti, "Design and performance analysis of uniform meander structured RF MEMS capacitive shunt switch along with perforations," *Microsyst. Technol.*, vol. 24, no. 2, pp. 901–908, Feb. 2018.

[17] E. Buitrago, M. F.-B. Badia, and A. M. Ionescu, "RF MEMS shunt capacitive switches using AlN compared toSi_3N_4dielectric," *J. Microelectromech. Syst.*, vol. 21, no. 5, pp. 1229–140, Oct. 2012.

[18] I.-J. Cho and E. Yoon, "Design and fabrication of a single membrane push-pull SPDT RF MEMS switch operated by electromagnetic actuation and electrostatic hold," *J. Micromachics Micro Eng.*, vol. 20, no. 3, pp. 1–8, Mar. 2010.

[19] T. Singh, K. N. Khaira, and S. J. Sengar, "Stress analysis using finite element modeling of a Novel RF microelectromechanical system shunt switch designed on quartz substrate for low voltage," *Trans. Electric Electron. Mater.*, vol. 1, pp. 225–230, Sep. 2013.

[20] Y. Jae, H. Kim, K. W. Chung, and U. B. Jong, "Monolithically integrated micromachined RF MEMS capacitive switches," *Sens. Actuators A, Phys.*, vol. 89, nos. 1–2, pp. 88–94, Mar. 2001.

[21] M. Angira and K. Rangra, "Design and investigation of a low insertion loss, broadband, enhanced self and hold down power RF-MEMS switch," *Microsyst. Technol.*, vol. 21, no. 6, pp. 1173–1178, Jun. 2015.

[22] D. Debajit and N. Chattoraj, "RF MEMS capacitive type shunt switch," in *Proc. IEEE Appl. Electromagn. Conf. (AEMC)*, Dec. 2013, pp. 145–185. doi: 10.1109/aemc.2013.7045081.

[23] P. Verma and S. Singh, "Design and simulation of RF MEMS capacitive type shunt switch & its major applications," *IOSR J. Electron. Commun. Eng.*, vol. 4, no. 5, pp. 60–68, Jan. 2013.

[24] L. H. Goldsmith, Z. Yao, S. Eshelman, and S. D. Denniston, "Performance of low-loss RF MEMS capacitive switches," *IEEE Microw. Guided Wave Lett.*, vol. 8, no. 8, pp. 269–271, Aug. 1998.
[25] F. DM, L. XH, Q. Yuan, and Z. HX, "Effect of etch holes on the capacitance and pull-in voltage in MEMS tunable capacitors," *Int. J. Electron.*, vol. 97, no. 12, pp. 1439–1448, 2010.
[26] P. G. Steeneken, T. G. Rijks, J. T. van Beek, M. J. Ulenaers, J. de Coster, and R. Puers, "Dynamics and squeeze film gas damping of a capacitive RF MEMS switch," *J. Micromech. Micro Eng.*, vol. 15, no. 1, p 176, Oct. 2004.

K. GIRIJA SRAVANI was born in India. She received the bachelor's degree in electronics and communication engineering and the master's degree in VLSI and embedded systems from JNTUK. She is currently pursuing the Ph.D. degree in MEMS research domain with the National Institute of Technology, Silchar. She is currently an Assistant Professor with the Department of Electronics and Communication Engineering, Koneru Lakshmaiah Education Foundation, Guntur, India. His current research interests include MEMS and RF MEMS. She is also working on MEMS project worth of 40 Lakhs funded by SERB, Goverentment of India. She has published more than 25 International research publications and presented more than five conference technical papers around the world.

D. PRATHYUSHA was born in India. She received the bachelor's degree in electronics and communication engineering from SCSVMV University, Kancheepuram, in 2016. She is currently pursuing the master's degree in VLSI with the Department of Electronics and Communication Engineering, Koneru Lakshmaiah Education Foundation, Guntur, India. She is currently doing project in area of MEMS. She has attended one conference and published a paper and one paper is under the review in Springer.

K. SRINIVASA RAO (M'17) was born in India. He received the master's and Ph.D. degrees from Central University. He is currently a Professor and the Head of the Microelectronics Research Group, Department of Electronics and Communication Engineering, Koneru Lakshmaiah Education Foundation, Guntur, India. His current research interests include MEMS-based reconfigurable antenna's actuators, bio-MEMS, RF MEMS switches, and RF MEMS Filters. He is also working on MEMS project worth of 40 Lakhs funded by SERB, Government of India. He has published more than 94 international research publications and presented more than 45 conference technical papers around the world. He is collaborated research work with NIT's, Central Universities, IIT's, and so on. Three Ph.D. Scholars has been Awarded under his Guidelines and seven Ph.D. Scholars are currently working with him. He is member of IETE and ISTE. He received the Young Scientist Award from the Department of Science and Technology, Government of India, in 2011. He also received UGC Major Research Project, in 2012. He received the Early career research Award from SERB, Government of India, in 2016.

P. ASHOK KUMAR was born in India. He received the bachelor's degree in electronics and communication engineering from JNTUH, in 2012, and the master's degree in VLSI from Koneru Lakshmaiah Education Foundation, in 2017, where he is currently pursuing Ph.D. degree in MEMS research domain. He has published 20 International research publications and presented more than five conference technical papers around the world.

G. SAI LAKSHMI was born in India. She received the bachelor's degree in electronics and instrumentation engineering from JNTUK, in 2016. She is currently pursuing the master's degree in VLSI with the Department of Electronics and Communication Engineering, Koneru Lakshmaiah Education Foundation, Guntur, India. She is currently doing project in the area of MEMS. She has attended one conference and published a paper and one paper is under the review in Springer.

CH. GOPI CHAND was born in India. He received the bachelor's degree in electronics and communication engineering from JNTUK, in 2016. He is currently pursuing the master's degree in VLSI with the Department of Electronics and Communication Engineering, Koneru Lakshmaiah Education Foundation, Guntur, India. He is currently doing project in area of MEMS. He has attended one conference and published a paper and one paper is under the review in Springer.

P. NAVEENA was born in India. She received the bachelor's degree in electronics and communication engineering from Vignan's Foundation for Science, Technology and Research (Deemed to be University), in 2016. She is currently pursuing the master's degree in VLSI with the Department of Electronics and Communication Engineering, Koneru Lakshmaiah Education Foundation, Guntur, India. She is currently doing project in the area of MEMS. She has attended one conference and published a paper and one paper is under the review in Springer.

LAKSHMI NARAYANA THALLURI (M) was born in India. He received the bachelor's degree in electronics and communication engineering from JNTUK, in 2009, and the master's degree in VLSI from Koneru Lakshmaiah Education Foundation, Guntur, India, in 2012, where he is currently pursuing the part time Ph.D. degree. He is also an Assistant Professor with the Department of Electronics and Communication Engineering, Andhra Loyola Institute of Engineering Technology, Vijayawada, India. His current research interests include RF MEMS switches, the Internet of Things, and digital system design. He is member of IE and IACSIT.

KOUSHIK GUHA (M) received the B.Tech. degree in electronics and communication engineering from Techno India, Salt Lake, Kolkata, under the West Bengal University of Technology, India, in 2005, the M.Tech. degree in electronics and communication engineering (RF and Microwaves) from Burdwan University, West Bengal, India, in 2007, and the Ph.D. degree in design and modeling of RF MEMS shunt switch from NIT Silchar, in 2016. He was a Lecturer with the Department of ECE, Haldia Institute of Technology (HIT), West Bengal, from 2007 to 2010. He has been an Assistant Professor with the Electronics and Communication Engineering Department, National Institute of Technology, Silchar, since 2010. He served as a Visiting Faculty of NIT Mizoram, from 2012 to 2014. He is a member of IETE.